



On the retrieval of the effective temperature of the ozone profile from ground-based spectroradiometric measurements

Peter Kiedron and Joseph Michalsky

Boulder, Colorado, USA

Fundamental uncertainty of ozone measurements

Ozone column abundance from Dobson and Brewer spectroradiometers is obtained from extinction measurements at a few discrete wavelengths. In the Brewer four wavelengths are used to obtain a closed-form linear analytic expression to derive ozone column:

$$DU = XSC \times [f(\lambda_1, \lambda_2, \lambda_3, \lambda_4) - ETC] / m_{O_3}$$

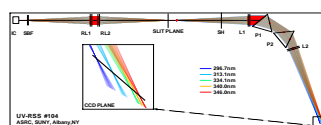
where $f(\lambda)$ is a linear combination of logarithms of four signals at four different wavelengths, XSC is the ozone cross-section, ETC is the extraterrestrial constant and m_{O_3} is ozone airmass. The wavelengths are selected in such a way as to cancel the effect of the unknown aerosol optical depth. This necessitates using the regions of the Huggins bands where the ozone cross-section happens to have the strongest temperature dependence. It is impossible to design ozone profile retrievals that are temperature independent using only four wavelengths [Thomas and Holland 1997]. The ozone profile has temporal, geographic and seasonal variability [Rood and Douglas 1985; Douglass et al. 1985; Randel and Cobb 1994]. Anomalous retrievals with a Brewer in Rome, Italy, were attributed to unstable and changing ozone profiles [Katasikas et al. 1995]. Dobsons and Brewers use Bass and Paur cross-sections at 227K and 229K, respectively. Dobson and Brewer results cannot accurately reflect ozone column changes because assumed temperatures do not always reflect the actual ozone profile temperatures. Even the small difference of 2K between the two methods leads to incongruent retrievals between the two types of instruments. The discrepancies usually have an annual cycle. The differences between Dobson and Brewers were reported at various sites, e.g., Toronto, Canada [Kerr et al. 1988], Hradec Kralove, Czech Republic [Vanecek 2006], Arosa, Switzerland [Scarnato et al. 2008]. Since at a given time and location there is only one ozone column, the Dobson and Brewer cannot both be right. More likely both are wrong. While annual cyclic differences are easier to explain and reconcile, a discrepancy that introduces a divergent trend may have more significant ramifications for ozone recovery and climate change issues. Is an ozone column trend caused by ozone change, atmospheric temperature change, or ozone column profile shape change? These are very important questions, however, they cannot be answered with current remote sensing ground-based instruments. Only colocated ozonesonde launches can resolve it. When sonde results are available, they can facilitate remote sensing retrievals at large solar zenith angles [Bernhard et al. 2005]. Unlike Dobson and Brewer networks, satellite-based retrievals use climatological ozone profiles in ozone column retrievals [McPeters et al. 2007]. While this seems to be a move in the right direction, the *a priori* information still raises the question about its influence on the final retrieval. What errors are introduced because of a faulty climatology? How does the retrieved variable respond to climatic changes that are not captured by the static *a priori* climatology?

Ozone profile uncertainty enters into the retrieved vertical ozone column as an error through two pathways: effective temperature of the ozone cross-section $\sigma(\lambda, T)$ and the unknown airmass $m_{O_3}(t)$. The latter error increases with solar zenith angle 0. The airmass uncertainty does not affect the slant path ozone column. However, for high, polar latitude regions the accurate retrieval of vertical ozone column with ground based spectroradiometers is practically impossible without ozonesonde data. In principle, the effective ozone temperature can be retrieved using wavelength-dependent transmission from other parts of the spectrum. When the temperature is known then appropriate ozone cross-sections can be used, and the temperature part of the uncertainty of ozone profile can be eliminated. However, for large solar zenith angles the uncertainty of ozone airmass remains.

A modified, multi-wavelength Brewer routine was successfully tried on Mauna Loa, Hawaii, and in the more problematic location (due to aerosols) of Toronto, Canada [Kerr 2002]. In this method the Brewer performed nine consecutive measurements to acquire direct irradiance at 45 wavelengths (five slits times nine grating positions). A modified sampling technique was used to allow acquisition of all 45 measurements in a relatively short time (2.5 minutes) as opposed to standard Brewer ozone measurements with five slits and one grating position only (repeated five times) that lasts over 3 minutes. This new technique is not widely used in the Brewer community. However, the multi-wavelength measurements can be more easily performed using a spectrograph with a detector array rather than using a scanning spectrometer with a single detector.

Rotating Shadowband Spectroradiometer (RSS)

The Rotating Shadowband Spectroradiometer (RSS) was developed at the Atmospheric Sciences Research Center (ASRC) at the State University of New York at Albany. Two versions were developed. The VIS-NIR measures direct and diffuse irradiances in the 360–1050 nm spectral range and the UV version covers 297–385 nm [Kiedron et al. 2002]. Its resolution varies from $\text{fwhm} = 0.311$ nm at 300 nm to $\text{fwhm} = 0.613$ nm at 380 nm. Its stray light – measured with a Cd-He 325 nm laser – is better than 0.5×10^{-6} . Measurements at the shortest wavelengths are noise-limited rather than stray-light limited, so the cut-on at 297 nm is noise-limited, and the cut-off at 385 nm is defined by a Hoya U-340 filter. The UV-RSS uses a double-prism refractive spectrograph. The spectrum is registered on 2D CCD array.



Ray tracing of RSS spectrograph



The fore optics uses a Teflon cosine diffuser. Once every minute the shadowband performs five measurements: Dark with closed shutter, Unblocked with band below horizon, Corr measurement with the band 9° before the sun beam, Blocked when sun beam is completely obstructed and Corr' 9° past the sun. Derived diffuse and direct signals using "shadowbanding algebra" are divided by cosine correction factors.



$$\begin{aligned} I_{\text{Diffuse}} &= [\text{Unblocked} - \frac{1}{2}(\text{Cor}' + \text{Cor}) + \text{Blocked}] / A_{\text{Diff}} \\ I_{\text{Direct}} &= \frac{1}{2}(\text{Cor}' + \text{Cor}) - \text{Blocked} / A_{\text{Dir}}(\alpha, \zeta) \\ I_{\text{Total}} &= I_{\text{Diffuse}} + I_{\text{Direct}} \end{aligned}$$

Shadowbanding algebra

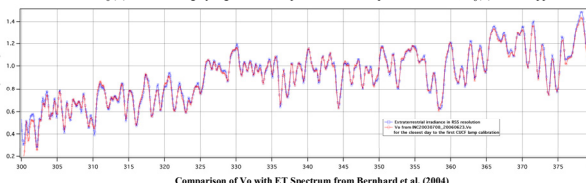


Calibration and performance of RSS

The RSS is calibrated using Langley regressions. The Langley regression analysis is performed on the 369 nm wavelength (808 pixels) in the 1 to 4 air mass range. This is used to select a viable Langley plot. To maintain the coherence between wavelengths the scans from the mask are used in the regressions for all the other wavelengths. However, due to poor signal-to-noise ratios at the shortest wavelengths, some scans for larger air masses are omitted in the regressions. The calibration constant $V_0(\lambda)$ is obtained by solving the linear regression equation

$$\ln(V(\lambda) + DU_{\text{air}} \cdot \sigma_v(\lambda) \cdot m_{O_3}(t)) + \tau_x(\lambda) \cdot m_{O_3}(t) = \ln\left(\frac{r^{\lambda}}{r^{\lambda} + r}\right) - \tau_{\text{air}}(\lambda) \cdot m_{O_3}(t)$$

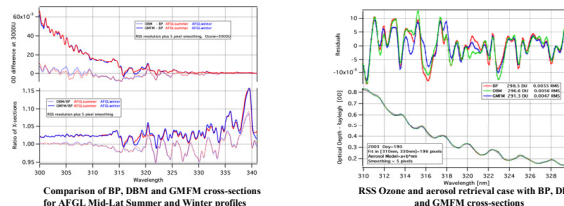
where r is Earth-Sun distance. It is essential to use a ozone column estimate DU_{air} to obtain correct values of $V_0(\lambda)$. We also correct for pressure that affects Rayleigh optical depth. The abscissa in the Langley plot is aerosol airmass. We use a standard H_2O vapor profile as a surrogate for the unknown aerosol air mass profile. The best test for the quality of results is comparison with extraterrestrial irradiance $I_0(\lambda)$. When Langley regressions are performed on lamp calibrated data, $V_0(\lambda)$ should approximate $I_0(\lambda)$.



Recently, direct and diffuse transmittances (T_{dir} and T_{dif}) obtained with the RSS and derived using $V_0(\lambda)$ from Langley regressions were compared with transmittances calculated with the TUV model for various cases of AOD, SSA, SA, g and SZA for data when the RSS was deployed at the ARM site in Oklahoma in May 2003 [Michalsky and Kiedron 2008].

Empirical ozone cross-sections

Consistency of ozone retrievals is hindered by the uncertainty in the empirical ozone cross-sections. We use three sources of ozone cross-sections: Bass-Paur (labeled BP) [Bass and Paur 1985, Paur and Bass 1985], Daumont-Brion-Malick (labeled DBM) [Daumont et al. 1992, Brion et al. 1993, Malick et al. 1995] and the GOME flight model (labeled GMFM) [Burrows et al. 1999]. The acronyms BP, DBM and GMFM are adopted from Liu et al. [2007]. The cross-sections have been used in ozone column and AOD retrievals from several years of RSS data at Table Mountain, Colorado [Kiedron et al. 2006]. With respect to BP based retrievals, DBM underestimates ozone by 2.5 DU and GMFM underestimates ozone by 7.4 DU on average in 5411 tested cases. These biases are reflected in retrieved aerosol optical depths. The retrievals were performed in the 310–330 nm window. A more complex picture of biases among cross-sections emerged from retrievals based on GOME data by Liu et al. [2007]. While GMFM yields systematic lower retrievals by 7–10 DU than BP and DBM, the differences are dependent on latitude and the fitting window. Unlike in RSS studies where the RMS residuals for all three cross-sections are comparable, in GOME retrievals with DBM yields significantly lower RMS than BP and GMFM.



A physical model of ozone temperature is not known, thus, the empirical cross-sections are parameterized using the least squares quadratic model that first was used with BP cross-sections:

$$\sigma_v(\lambda, T) = c_1(\lambda) + c_2(\lambda) \cdot T + c_3(\lambda) \cdot T^2$$

The equations that have semblance of physical justification like: $\sigma_v(\lambda, T) = a(\lambda) \cdot b(\lambda) \cdot \exp(-c/T)$ or $\sigma_v(\lambda, T) = \lambda^{-1} \cdot a(\lambda) \cdot \exp[b(\lambda)/T + c(\lambda)] \cdot T$ were found to be inadequate to fit empirical data [Orphal, 2003]. Furthermore, some empirical spectra appear to be outliers. Liu et al. [2007] found that the 273K DBM spectrum introduces large residuals in the quadratic fit.

Ozone profile cross-section

As long as radiation is quasi-monochromatic the Beer-Lambert-Bouguer law holds for the refractively-curved path throughout the ozone profile: $I(\lambda, t) = I_0(\lambda) \cdot \exp[-DU_{\text{air}} \cdot \sigma_v(\lambda, t) \cdot m_{O_3}(t)]$, where $\sigma_v(\lambda)$ is the ozone profile cross-section and the ozone airmass $m_{O_3}(t)$ is independent of ozone cross-section. Let us define normalized (integral is unity) vertical ozone profile $p(z)$, vertical temperature profile $T(z)$, air index of refraction profile $n(z)$, elevation z , Earth radius R and apparent solar zenith angle θ at the observation point. Then $\sigma_v(\lambda)$ and $m_{O_3}(t)$ can be derived from formulas that one can find in [Thomason et al. 1983]:

$$\sigma_v(\lambda) = \frac{1}{m_{O_3}(t)} \int_{\lambda}^{\infty} \frac{\sigma_v(\lambda, T(z)) p(z)}{1 - \left[\frac{n(z, R+z)}{n(z, R+z)} \sin^2 \theta \right]} dz \quad \text{and} \quad m_{O_3}(t) = \int_{\lambda}^{\infty} \frac{p(z)}{1 - \left[\frac{n(z, R+z)}{n(z, R+z)} \sin^2 \theta \right]} dz$$

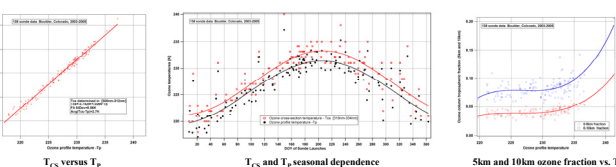
By definition $m_{O_3}(0) = 1$. In spectral regions where $d\sigma_v(\lambda, T)/dT \approx 0$ the profile cross-section $\sigma_v(\lambda)$ is independent of t , but where the temperature dependence is not negligible $\sigma_v(\lambda)$ has a solar zenith angle dependent component. For $0 < \theta < 80^\circ$ for typical profiles this component is less than 0.1% and thus can be ignored. However, for large solar zenith angles $0 > 80^\circ$ one must bear in mind that the ozone profile cross-section $\sigma_v(\lambda)$ is 0 dependent. Furthermore, it is important to remember that with the exception of single layer profiles defined such that, $p(z) \propto (z-h)$, the profile cross-section may not be equal to ozone cross-section for any temperature. The degree with which $\sigma_v(\lambda, T)$ may approximate $\sigma_v(\lambda)$ also depends on the spectral window.

Ozone profile and ozone cross-section temperatures

There is no unique definition of temperature associated with the ozone profile. Commonly, e.g., Scarnato et al. [2008], the first moment T_p of temperature $T(z)$ is used as the definition of ozone profile temperature. T_p , however, does not reflect the effective temperature of the ozone profile cross-section $\sigma_v(\lambda, t)$, and, thus, it is not sufficiently accurate to use in retrievals. A better definition is the temperature of the cross-section $\sigma_v(\lambda, T)$ that approximates $\sigma_v(\lambda)$ the best in a given spectral range. This temperature we call ozone profile cross-section temperature T_{CS} :

$$T_p = \frac{1}{t} \int_t^{\infty} T(z) p(z) dz \quad T_{CS} = \min_{\lambda} \int_{\lambda}^{\infty} |\sigma_v(\lambda, T) - \sigma_v(\lambda, T_p)|^2 d\lambda$$

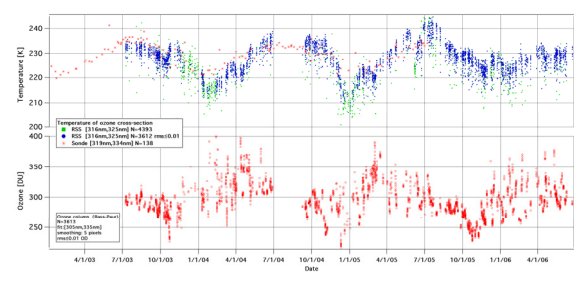
T_p and T_{CS} are not equal. They correlate with each other, but there is no functional dependence between them within the broad set of possible profiles.



T_{CS} depends on the spectral range $[\lambda_1, \lambda_2]$. For instance, for profiles encountered at Table Mountain in Boulder, Colorado, T_{CS} for [319–334 nm] is on average larger by 0.45K than T_p for [300–312 nm] for BP cross-sections in RSS resolution. Ozone profile cross-section temperature T_{CS} is on average 2.7K higher than ozone profile temperature T_p . In some cases the ozone profile temperature can indicate the ozone distribution; for example, the ratio of tropospheric ozone column to the total ozone column. However, with the exception of a few extreme cases there is no correlation (see figure above) between ozone tropospheric fraction and ozone profile temperature. Nevertheless the ability to retrieve the ozone profile cross-section can be used to detect anomalous profiles.

Ozone temperature retrievals

Ozone column for 3211 (rms < 0.01OD) scans (10 scans per day for airmasses less than 4) was retrieved using BP cross-sections by the method described in Kiedron et al. [2006]. Linear dependence of aerosols on wavelength was assumed. The estimate of ozone cross-section $\sigma_{RSS}(\lambda)$ was compared with $\sigma_{BP}(\lambda, T)$ for $200\text{K} \leq T \leq 250\text{K}$ in [316–325 nm] range. The T_{CS} was defined as the one that produced the smallest rms between $\sigma_{RSS}(\lambda)$ and $\sigma_{BP}(\lambda, T)$. Different spectral intervals produce different temperatures that correlate with others well, but have small biases with respect to each other. A trial run of ozone retrievals that incorporates the knowledge of T_{CS} (not shown here) resulted only in small ozone adjustments because the ozone retrieval method used here already utilizes climatologically based ozone cross-sections. DBM and GMFM cross-sections were not tested.



References

- [1977] Thomas, R. W. L. and Holland, A.C., "Ozone estimates derived from Dobson direct sun measurements: effect of atmospheric temperature variations and scattering," *Appl. Opt.* **16**, 613–618, 1977.
- [1980] Thomason, L. W., Herman, B. M. and Reagan, J. A., "The effect of atmospheric attenuators with structured vertical distributions on air mass determinations and Langley plot analyses," *J. Atmos. Sci.* **40**, 1851–1862, 1983.
- [1982] Rood, R.B., Douglas, A.R., and Stader, R.S., "Interpretation of Ozone Temperature Correlations. 2. Analysis of TUVE Ozone Data," *J. Geophys. Res.* **90**, 10,693–10,708, 1982.
- [1985] Douglass, A.R., Rood, R.B., Stader, R.S., "Interpretation of Ozone Temperature Correlations. 1. Theory," *J. Geophys. Res.* **90**, 11,289–11,400, 1985.
- [1988] Kerr, J. B., Adridge, J. A., and Evans, W. F. J., "Intercomparison of total ozone measured by the Brewer and Dobson Spectrophotometers at Toronto," *J. Geophys. Res.* **93**(11), 11,291–11,400, 1988.
- [1992] Daumont, R.B., Brion, J., and Malick, J., "UV-Ozone Spectroscopy. I. Absorption cross-sections at room temperature," *J. Atmos. Chem.* **15**, 145–155, 1992.
- [1994] Brion, J., and Malick, J., "UV-Ozone Spectroscopy. II. Absorption cross-sections and temperature dependence," *J. Atmos. Chem.* **19**, 613–622, 1994.
- [1995] Malick, J., Daumont, D., Charbonneau, J., Patrice, C., Chakir, A., and Brion, J., "Ozone UV-spectroscopy. III. Absorption cross-sections and temperature dependence," *J. Atmos. Chem.* **21**, 263–273, 1995.
- [1996] Brion, J., and Malick, J., "UV-Ozone Spectroscopy. IV. Investigation of a peculiar asymptotic behavior at Rome," *J. Atmos. Chem.* **21**, 275–285, 1995.
- [1998] Brion, J., and Malick, J., "UV-Ozone Spectroscopy. V. A Comparison of Dobson and Brewer Spectrophotometers," *J. Atmos. Chem.* **21**, 287–297, 1995.
- [1999] Brion, J., and Malick, J., "UV-Ozone Spectroscopy. VI. A Comparison of Dobson and Brewer Spectrophotometers," *J. Atmos. Chem.* **21**, 299–311, 1995.
- [2000] Brion, J., and Malick, J., "UV-Ozone Spectroscopy. VII. A Comparison of Dobson and Brewer Spectrophotometers," *J. Atmos. Chem.* **21**, 313–321, 1995.
- [2002] Kerr, J. B., Dobson, J., and Brion, J., "A Comparison of Dobson and Brewer Spectrophotometers," *J. Geophys. Res.* **107**, 10,629, 2002.
- [2003] Kiedron, P., and Michalsky, J., "A Comparison of Dobson and Brewer Spectrophotometers," *J. Geophys. Res.* **108**, 10,629, 2003.
- [2004] Kiedron, P., and Michalsky, J., "A Comparison of Dobson and Brewer Spectrophotometers," *J. Geophys. Res.* **109**, 10,629, 2004.
- [2005] Kiedron, P., and Michalsky, J., "A Comparison of Dobson and Brewer Spectrophotometers," *J. Geophys. Res.* **110**, 10,629, 2005.
- [2006] Kiedron, P., and Michalsky, J., "A Comparison of Dobson and Brewer Spectrophotometers," *J. Geophys. Res.* **111**, 10,629, 2006.
- [2007] Kiedron, P., and Michalsky, J., "A Comparison of Dobson and Brewer Spectrophotometers," *J. Geophys. Res.* **112**, 10,629, 2007.
- [2008] Kiedron, P., and Michalsky, J., "A Comparison of Dobson and Brewer Spectrophotometers," *J. Geophys. Res.* **113**, 10,629, 2008.
- [2009] Kiedron, P., and Michalsky, J., "A Comparison of Dobson and Brewer Spectrophotometers," *J. Geophys. Res.* **114**, 10,629, 2009.
- [2010] Kiedron, P., and Michalsky, J., "A Comparison of Dobson and Brewer Spectrophotometers," *J. Geophys. Res.* **115**, 10,629, 2010.
- [2011] Kiedron, P., and Michalsky, J., "A Comparison of Dobson and Brewer Spectrophotometers," *J. Geophys. Res.* **116**, 10,629, 2011.
- [2012] Kiedron, P., and Michalsky, J., "A Comparison of Dobson and Brewer Spectrophotometers," *J. Geophys. Res.* **117**, 10,629, 2012.
- [2013] Kiedron, P., and Michalsky, J., "A Comparison of Dobson and Brewer Spectrophotometers," *J. Geophys. Res.* **118**, 10,629, 2013.
- [2014] Kiedron, P., and Michalsky, J., "A Comparison of Dobson and Brewer Spectrophotometers," *J. Geophys. Res.* **119**, 10,629, 2014.
- [2015] Kiedron, P., and Michalsky, J., "A Comparison of Dobson and Brewer Spectrophotometers," *J. Geophys. Res.* **120**, 10,629, 2015.
- [2016] Kiedron, P., and Michalsky, J., "A Comparison of Dobson and Brewer Spectrophotometers," *J. Geophys. Res.* **121**, 10,629, 2016.
- [2017] Kiedron, P., and Michalsky, J., "A Comparison of Dobson and Brewer Spectrophotometers," *J. Geophys. Res.* **122**, 10,629, 2017.
- [2018] Kiedron, P., and Michalsky, J., "A Comparison of Dobson and Brewer Spectrophotometers," *J. Geophys. Res.* **123**, 10,629, 2018.
- [2019] Kiedron, P., and Michalsky, J., "A Comparison of Dobson and Brewer Spectrophotometers," *J. Geophys. Res.* **124**, 10,629, 2019.
- [2020] Kiedron, P., and Michalsky, J., "A Comparison of Dobson and Brewer Spectrophotometers," *J. Geophys. Res.* **125**, 10,629, 2020.
- [2021] Kiedron, P., and Michalsky, J., "A Comparison of Dobson and Brewer Spectrophotometers," *J. Geophys. Res.* **126**, 10,629, 2021.
- [2022] Kiedron, P., and Michalsky, J., "A Comparison of Dobson and Brewer Spectrophotometers," *J. Geophys. Res.* **127**, 10,629, 2022.
- [2023] Kiedron, P., and Michalsky, J., "A Comparison of Dobson and Brewer Spectrophotometers," *J. Geophys. Res.* **128**, 10,629, 2023.
- [2024] Kiedron, P., and Michalsky, J., "A Comparison of Dobson and Brewer Spectrophotometers," *J. Geophys. Res.* **129**, 10,629, 2024.
- [2025] Kiedron, P., and Michalsky, J., "A Comparison of Dobson and Brewer Spectrophotometers," *J. Geophys. Res.* **130**, 10,629, 2025.
- [2026] Kiedron, P., and Michalsky, J., "A Comparison of Dobson and Brewer Spectrophotometers," *J. Geophys. Res.* **131**, 10,629, 2026.
- [2027] Kiedron, P., and Michalsky, J., "A Comparison of Dobson and Brewer Spectrophotometers," *J. Geophys. Res.* **132**, 10,629, 2027.
- [2028] Kiedron, P., and Michalsky, J., "A Comparison of Dobson and Brewer Spectrophotometers," *J. Geophys. Res.* **133**, 10,629, 2028.
- [2029] Kiedron, P., and Michalsky, J., "A Comparison of Dobson and Brewer Spectrophotometers," *J. Geophys. Res.* **134**, 10,629, 2029.
- [2030] Kiedron, P., and Michalsky, J., "A Comparison of Dobson and Brewer Spectrophotometers," *J. Geophys. Res.* **135**, 10,629, 2030.
- [2031] Kiedron, P., and Michalsky, J., "A Comparison of Dobson and Brewer Spectrophotometers," *J. Geophys. Res.* **136**, 10,629, 2031.
- [2032] Kiedron, P., and Michalsky, J., "A Comparison of Dobson and Brewer Spectrophotometers," *J. Geophys. Res.* **137**, 10,629, 2032.
- [2033] Kiedron, P., and Michalsky, J., "A Comparison of Dobson and Brewer Spectrophotometers," *J. Geophys. Res.* **138**, 10,629, 2033.
- [2034] Kiedron, P., and Michalsky, J., "A Comparison of Dobson and Brewer Spectrophotometers," *J. Geophys. Res.* **139**, 10,629, 2034.
- [2035] Kiedron, P., and Michalsky, J., "A Comparison of Dobson and Brewer Spectrophotometers," *J. Geophys. Res.* **140**, 10,629, 2035.
- [2036] Kiedron, P., and Michalsky, J., "A Comparison of Dobson and Brewer Spectrophotometers," *J. Geophys. Res.* **141**, 10,629, 2036.
- [2037] Kiedron, P., and Michalsky, J., "A Comparison of Dobson and Brewer Spectrophotometers," *J. Geophys. Res.* **142**, 10,629, 2037.
- [2038] Kiedron, P., and Michalsky, J., "A Comparison of Dobson and Brewer Spectrophotometers," *J. Geophys. Res.* **143**, 10,629, 2038.
- [2039] Kiedron, P., and Michalsky, J., "A Comparison of Dobson and Brewer Spectrophotometers," *J. Geophys. Res.* **144**, 10,629, 2039.
- [2040] Kiedron, P., and Michalsky, J., "A Comparison of Dobson and Brewer Spectrophotometers," *J. Geophys. Res.* **145**, 10,629, 2040.
- [2041] Kiedron, P., and Michalsky, J., "A Comparison of Dobson and Brewer Spectrophotometers," *J. Geophys. Res.* **146**, 10,629, 2041.
- [2042] Kiedron, P., and Michalsky, J., "A Comparison of Dobson and Brewer Spectrophotometers," *J. Geophys. Res.* **147**, 10,629, 2042.
- [2043] Kiedron, P., and Michalsky, J., "A Comparison of Dobson and Brewer Spectrophotometers," *J. Geophys. Res.* **148**, 10,629, 2043.
- [2044] Kiedron, P., and Michalsky, J., "A Comparison of Dobson and Brewer Spectrophotometers," *J. Geophys. Res.* **149**, 10,629, 2044.
- [2045] Kiedron, P., and Michalsky, J., "A Comparison of Dobson and Brewer Spectrophotometers," *J. Geophys. Res.* **150**, 10,629, 2045.
- [2046] Kiedron, P., and Michalsky, J., "A Comparison of Dobson and Brewer Spectrophotometers," *J. Geophys. Res.* **151**, 10,629, 2046.
- [2047] Kiedron, P., and Michalsky, J., "A Comparison of Dobson and Brewer Spectrophotometers," *J. Geophys. Res.* **152**, 10,629, 2047.
- [2048] Kiedron, P., and Michalsky, J., "A Comparison of Dobson and Brewer Spectrophotometers," *J. Geophys. Res.* **153**, 10,629, 2048.
- [2049] Kiedron, P., and Michalsky, J., "A Comparison of Dobson and Brewer Spectrophotometers," *J. Geophys. Res.* **154**, 10,629, 2049.
- [2050] Kiedron, P., and Michalsky, J., "A Comparison of Dobson and Brewer Spectrophotometers," *J. Geophys. Res.* **155**, 10,629, 2050.
- [2051] Kiedron, P., and Michalsky, J., "A Comparison of Dobson and Brewer Spectrophotometers," *J. Geophys. Res.* **156**, 10,629, 2051.
- [2052] Kiedron, P., and Michalsky, J., "A Comparison of Dobson and Brewer Spectrophotometers," *J. Geophys. Res.* **157**, 10,629, 2052.
- [2053] Kiedron, P., and Michalsky, J., "A Comparison of Dobson and Brewer Spectrophotometers," *J. Geophys. Res.* **158**, 10,629, 2053.
- [2054] Kiedron, P., and Michalsky, J., "A Comparison of Dobson and Brewer Spectrophotometers," *J. Geophys. Res.* **159**, 10,629, 2054.
- [2055] Kiedron, P., and Michalsky, J., "A Comparison of Dobson and Brewer Spectrophotometers," *J. Geophys. Res.* **160**, 10,629, 2055.
- [2056] Kiedron, P., and Michalsky, J., "A Comparison of Dobson and Brewer Spectrophotometers," *J. Geophys. Res.* **161**, 10,629, 2056.
- [2057] Kiedron, P., and Michalsky, J., "A Comparison of Dobson and Brewer Spectrophotometers," *J. Geophys. Res.* **162**, 10,629, 2057.
- [2058] Kiedron, P., and Michalsky, J., "A Comparison of Dobson and Brewer Spectrophotometers," *J. Geophys. Res.* **163**, 10,629, 2058.
- [2059] Kiedron, P., and Michalsky, J., "A Comparison of Dobson and Brewer Spectrophotometers," *J. Geophys. Res.* **164**, 10,629, 2059.
- [2060] Kiedron, P., and Michalsky, J., "A Comparison of Dobson and Brewer Spectrophotometers," *J. Geophys. Res.</i*